CO₂ Emissions Reduction

Reduction of CO₂ Emission from Off-Gases of Steel Industry by Dry Reforming of Methane

Sofia D. Angeli, Sabrina Gossler, Sven Lichtenberg, Gilles Kass, Anand Kumar Agrawal, Miriam Valerius, Klaus Peter Kinzel, and Olaf Deutschmann*

Abstract: In a novel process, CO₂ and CH₄ from the off-gases of the coke oven and blast furnace are used in homogeneous reforming of those greenhouse gases to valuable syngas, a mixture of H₂ and CO. Synthetic mixtures of the off-gases from those large apparatuses of steel industry are fed to a high-temperature, high-pressure flow reactor at varying temperature, pressure, residence time, and mixing ratio of coke oven gas (COG) to blast furnace gas (BFG). In this study, a maximal reduction of 78.5 % CO₂ and a CH₄ conversion of 95 % could be achieved at 1350°C, 5.5 bar, and a COG/BFG ratio of 0.6. Significant carbonaceous deposits were formed but did not block the reactor tube in the operational time window allowing cyclic operation of the process. These measurements were based on prior thermodynamic analysis and kinetic predictions using an elementary-step reaction mechanism.

The steel industry is responsible for 7–9 % of the global direct CO₂ emissions.[1] Tremendous efforts are currently devoted to the development of technologies to reduce these emissions, for instance by the utilization of the off-gases.[2–5] These off-gases are the Coke Oven Gas (COG), Blast Furnace Gas (BFG), and Basic Oxygen Furnace Gas (BOFG) with typical compositions presented in Table 1.[4]

There are several ways to use these off-gases: directly as a fuel for power generation due to the occurrence of combustible compounds such as H₂, CO, and CH₄,[3,6–9] as reducing agents for iron oxides,[10] and separation and consecutive re-use of single components such as H₂ and CO from COG and BFG, respectively.[2,11,12] Furthermore, components of these off-gases can also be catalytically converted, such as CO of BFG to H₂ via the water–gas shift (WGS)

Table 1: Typical composition of the steel industry off-gases.[4]

Feed name	COG	BFG	BOFG
CH₄ (vol %)	22.0	0.0	0.0
CₓHᵧ (vol %)	2.0	0.0	0.0
CO₂ (vol %)	1.2	21.6	20.0
H₂O (vol %)	4.0	4.0	4.0
H₂ (vol %)	60.7	3.7	3.2
CO (vol %)	4.1	23.5	54.0
N₂ (vol %)	5.8	46.6	18.1
Ar + O₂ (vol %)	0.2	0.6	0.7

reaction [Eq. (1)], CH₄ of COG to syngas/H₂ via dry [Eq. (2)] and steam [Eq. (3)] reforming.[13–16]

$$CO + H_2O \rightarrow CO_2 + H_2 \quad \Delta H_{298K} = -41.2 \text{ kJ mol}^{-1} \quad (1)$$

$$CH_4 + CO_2 \rightarrow 2\,CO + 2\,H_2 \quad \Delta H_{298K} = 247.0 \text{ kJ mol}^{-1} \quad (2)$$

$$CH_4 + H_2O \rightarrow CO + 3\,H_2 \quad \Delta H_{298K} = 206.0 \text{ kJ mol}^{-1} \quad (3)$$
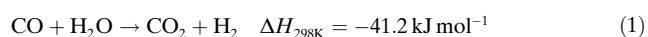
The produced syngas can be further used for the production of methanol, dimethylether, and other valuable chemicals.[17–19] However, it must be stressed that the steelwork off-gases contain traces of aromatic compounds, chloride, sulfur (mainly H₂S), and HCN, which all are potential catalyst poisons. Therefore, purification processes are required before feeding the gas streams over the catalysts, which increases costs and complexity of the process.[4]

The process presented here valorizes the off-gases COG and BFG. These off-gases are homogeneously converted to syngas (H₂ and CO) in a regenerative heat exchanger. The syngas is then used as reducing gas in the blast furnace (Scheme 1). The heat exchanger operates in two functional modes: In an initially hot period ("on blast"), the heat stored in the solid structure (stove) is used to drive the endothermic

[*] Dr. S. D. Angeli, S. Gossler, S. Lichtenberg, Prof. Dr. O. Deutschmann
Institute for Chemical Technology and Polymer Chemistry
Karlsruhe Institute of Technology (KIT)
76128 Kalrsruhe (Germany)
E-mail: deutschmann@kit.edu

G. Kass, A. K. Agrawal, M. Valerius, Dr.-Ing. K. P. Kinzel
PAUL WURTH SA
L-1122 Luxembourg (Luxembourg)

⊞ Supporting information and the ORCID identification number(s) for
ⓘ the author(s) of this article can be found under:
https://doi.org/10.1002/anie.202100577.
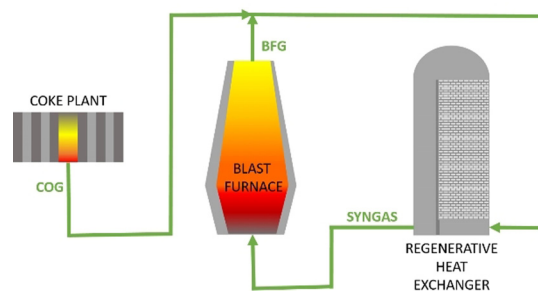
Scheme 1. Proposed process for utilization of ironmaking off-gases for syngas production in the hot period.

dry reforming. The time-dependent temperature profile of the regenerative heat exchanger is a process parameter which is a function of the inlet gas temperature, the gas flow rate and composition (COG/BFG ratio), and the initial temperature of the stove.[20] After the stove is cooled down, approximately after 30 minutes of syngas production, the operational mode switches to the cold period ("off blast"). In this initially cold mode the stove is reheated by burning BFG with air. The two streams, COG/BFG and BFG/air, are not in contact due to the periodic operation.

In our study, the reforming of COG and BFG in the absence of a catalyst was first studied by thermodynamic and kinetic analysis. For the simulation of the gas-phase reaction kinetics a detailed chemical model from literature was used.[21] Based on this modeling study, experiments were performed at the most promising conditions (temperature, pressure, residence time) relevant to the operation conditions of the heat exchanger. Three alternative mixing ratios of the two gas streams were investigated (Table 2).

The endothermic reforming reactions are thermodynamically favored at high temperatures. Methane is the main hydrocarbon in the feed and a high conversion is required for the process to be sustainable. The equilibrium conversion of methane higher than 90% is achieved at temperatures above 930–1050°C at the reference pressure of 5.5 bar, depending on the COG/BFG ratio (Figure 1). The conversion of steam and CO_2 is highly affected by the relative methane-to-oxidants ratio of each mixture. The mixture COG/BFG of 1.4 corresponds to a relative ratio of inlet carbon from

hydrocarbons to oxidants of 1 (Table 2). As the mixture is richer in BFG this relative hydrocarbons-to-oxidants ratio becomes lower than unity, which leads to low conversion of CO_2 and H_2O due to their excess in the feed. Additionally, the richer the mixture in BFG, the higher the content of CO in the feed, which in turn favors the formation of H_2O via the reverse water–gas shift (RWGS) reaction. The latter effect is dominant in the COG/BFG mixture ratio of 0.6, at which no H_2O conversion is expected by thermodynamics.

The formation of carbonaceous deposits can present a real technical challenge, since it might be accumulated in the heat exchanger and the pipes causing pressure drop or even clog the pipes. Thermodynamically, the formation of graphitic carbon is favored below 1000°C due to the exothermic reactions of CO and CO_2 hydrogenation [Eq. (4) and (5)] as well as the Boudouard reaction [Eq. (6), Figure 2].

$$H_2 + CO \rightarrow C + H_2O \quad \Delta H_{298K} = -131.3 \, kJ \, mol^{-1} \tag{4}$$

$$2\,H_2 + CO_2 \rightarrow C + 2\,H_2O \quad \Delta H_{298K} = -90.2 \, kJ \, mol^{-1} \tag{5}$$

$$2\,CO \rightarrow C + CO_2 \quad \Delta H_{298K} = -172.5 \, kJ \, mol^{-1} \tag{6}$$
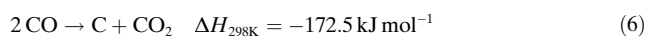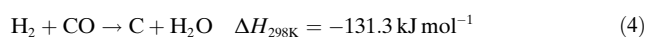
Even though the temperature in the heat exchanger is higher than 800°C, lower temperatures are expected in the inlet section, where the gas is progressively heated up. Therefore, the experimental investigation of the accumulation of carbonaceous deposits is a must when studying this process.

The typical pressure range of the heat exchanger is 3–5.5 bar. Therefore, the effect of pressure variation on the equilibrium composition was also investigated (Figure S1 of the Supporting Information). For instance, at a temperature of 1000°C the methane conversion is decreased as the pressure increases, reaching a minimum of 93% methane conversion at 7 bar. However, at higher temperatures the pressure barely affects the conversion of CH_4 as well as CO_2.

The thermodynamic analysis revealed the potential of dry reforming [Eq. (2)] in the gas phase under the typical conditions of the heat exchanger. Next, kinetic limitations
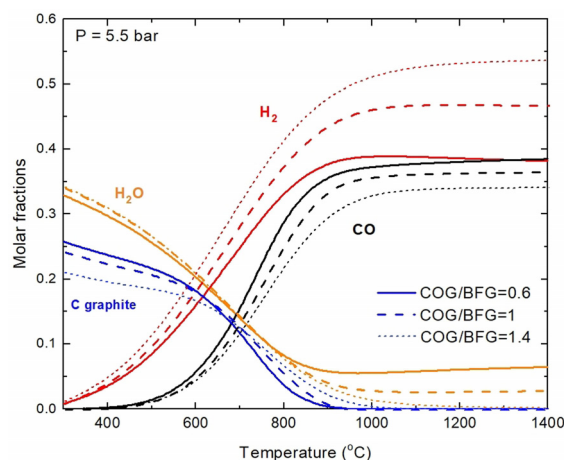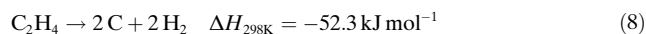
Table 2: Properties of the mixtures of COG and BFG considered.

	COG/BFG = 1.4	COG/BFG = 1	COG/BFG = 0.6
CH_4 (vol%)	12.57	10.77	8.62
C_2H_4 (vol%)	2.43	2.09	1.67
CO_2 (vol%)	13.37	15.49	18.03
H_2O (vol%)	3.83	4.00	4.20
H_2 (vol%)	37.30	33.88	29.78
CO (vol%)	15.26	17.11	19.33
N_2 (vol%)	15.24	16.66	18.36
$\frac{CH_4 + 2C_2H_4}{CO_2 + H_2O}$	1.00	0.76	0.53

Figure 1. Equilibrium conversion of COG/BFG mixtures at 5.5 bar.

Figure 2. Equilibrium composition at 5.5 bar including graphite formation.

had to be considered in order to investigate whether considerable conversion can be achieved under the operation conditions of the proposed regenerative heat exchanger. Therefore, we studied the chemical kinetics of the given mixtures by numerical simulations using a recently established elementary-step reaction mechanism named PolyMech.[21] PolyMech consists of 558 reactions among 83 species and was already applied to study chemical kinetics at conditions occurring in polygeneration devices.[22] Since the potential formation of carbonaceous deposits is an important technical issue, the mechanism includes not only reactions for the main products, but also all possible steps leading to the formation of coke precursors (alkenes, alkines, some aromatic species). These simulations confirmed that methane conversion over 90% can be achieved at temperatures higher than 1320°C at 5.5 bar (Figure 3). The conversion of ethylene was over 80% even at 600°C. For temperatures below 1100°C, the molar fraction of methane in the product stream is higher than the inlet stream, because of the processes of methanation [Eq. (7)] as well as decomposition of C_2H_4 [Eq. (8)] are thermodynamically favored in this temperature range.

$$4\,H_2 + CO_2 \rightarrow CH_4 + 2\,H_2O \quad \Delta H_{298K} = -164.9\,kJ\,mol^{-1} \tag{7}$$

$$C_2H_4 \rightarrow 2\,C + 2\,H_2 \quad \Delta H_{298K} = -52.3\,kJ\,mol^{-1} \tag{8}$$

For temperatures above 1100°C methane conversion increases drastically reaching values up to 96% at 1350°C (COG/BFG = 0.6). A temperature of 1130°C is required (COG/BFG = 1.4) to achieve 70% conversion of CO_2.

These simulations gave guidance to the operating conditions of the experimental part of this study, which was conducted in a temperature range of 900–1350°C and at pressures of 3 bar and 5.5 bar. Since the hot period of the heat exchanger is approximately 30 minutes, we studied the mixture in the tubular hot reactor for the same amount of time, in particular to also determine the amount of coke and soot that can be produced at the operating conditions of the heat exchanger. The experimentally measured dry outlet
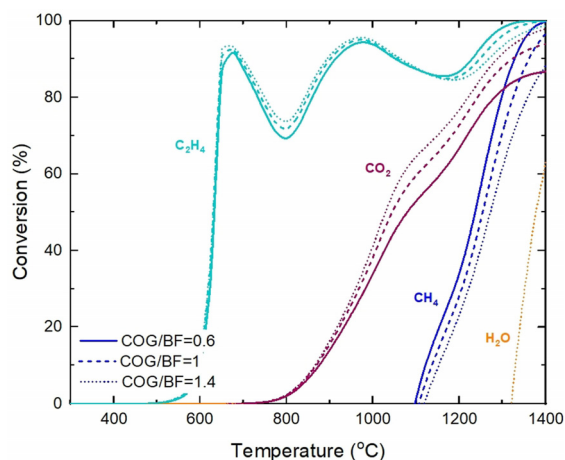
compositions at 5.5 bar are shown in Figures 4 and 5 for COG/BFG of 0.6 and 1.0, respectively.

It is shown that the outlet composition is not strongly affected by the inlet mixture, especially at lower temperatures. In the temperature range of 900–1050°C the methanation reaction [Eq. (7)] is dominant, which leads to increase in the molar fraction of CH_4 and simultaneous reduction of the molar fractions of CO_2 and H_2. At higher temperature the main products are CO and H_2 due to reforming reactions. At 1350°C, the dry outlet gas is composed of over 75% of syngas with a H_2/CO ratio of approximately 1.0. It should also be noted that the product mixture is far from reaching the thermodynamic equilibrium at temperatures below 1300°C (Figure S4). Further figures of the experimental results obtained at varying operating conditions are included in the Supporting Information (Figures S5–S11). The highest methane conversion was achieved for a mixture with the COG/BFG ratio of 0.6 at 5.5 bar, which can be understood by the higher concentration of oxidants compared to CH_4 and other hydrocarbons.
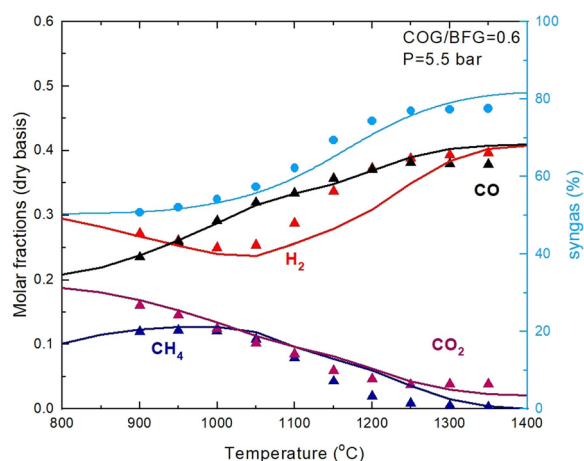

Figure 4. Experimental composition (dry basis) for COG/BFG = 0.6 at 5.5 bar. Points: experiment, line: simulation.

Figure 3. Conversion of COG/BFG mixtures at 5.5 bar predicted by the kinetic model.
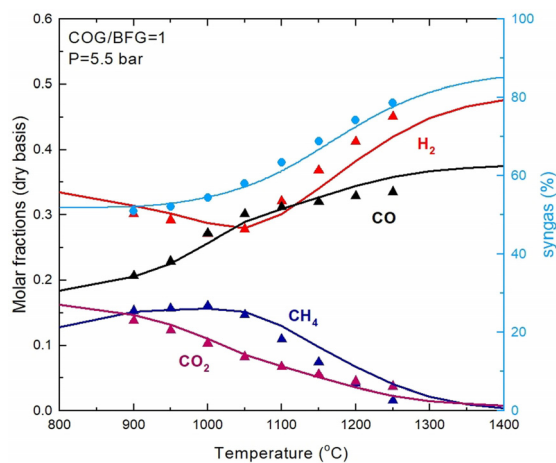

Figure 5. Experimental composition (dry basis) for COG/BFG = 1 at 5.5 bar. Points: experiment, line: simulation.

The good agreement of the experimentally measured and numerically predicted reactor outlet compositions reveals that the kinetic model used is able to depict the chemical reaction kinetics of methanation and reforming in the two temperature regimes quite well. The model also successfully predicts the change in the slope of H_2 and CH_4 molar fractions (Figures 4 and 5). Additionally, a very good agreement with the experimental data was found for the CO and CO_2 molar fractions, indicating that the equilibrium of the WGS reaction is also well considered by the kinetic model. The evaluation of the kinetic model against all experimental data obtained with the three inlet mixtures is shown in the parity plot included in the Supporting Information (Figure S12). Consequently, the kinetic model applied is a good basis for process simulations to scale up the technology proposed.

Apart from high CH_4 and CO_2 conversion, the already mentioned formation of carbonaceous deposits is of high relevance for the technical application. While the thermodynamic model can predict regions of the operating conditions in which coke formation matters, the used kinetic model is not able to do so, simply due to the fact that the kinetic model does not include reactions that lead to solid carbonaceous species. However, it is known that C_2H_4, C_2H_2, and C_6H_6 are precursors for soot formation, which lead to generic coke precursors, such as polyaromatic hydrocarbons (PAHs) due to hydrogen abstraction and carbon addition, the so-called HACA mechanism.[23,24] Therefore, in order to theoretically assess the tendency towards carbonaceous deposits, the formation of coke precursors such as C_2H_6, C_2H_4, C_2H_2, and C_6H_6 that are included in the model can serve as indicators for coke formation.[25] In Figure 6, the molar fractions of these species as predicted by the kinetic model are shown as a function of temperature for all three mixtures of COG and BFG. It is clear that the lower the initial concentration of C_2H_4 in the feed, the lower the molar fractions of the coke precursors in the outlet stream predicted by the model. As a result, the model suggests a COG/BF = 0.6 mixture for minimizing the formation of carbonaceous deposits.

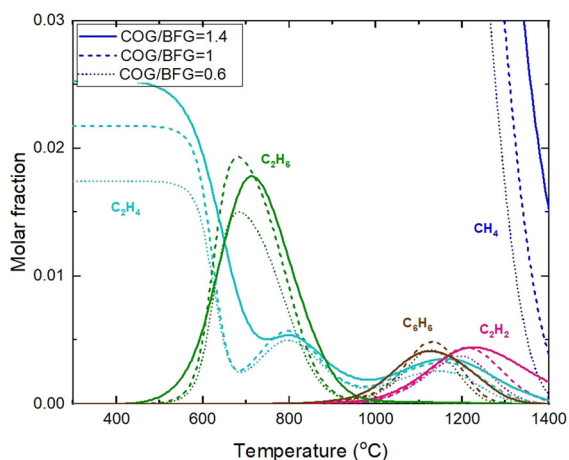The model predictions also suggest that coke formation may occur at cold spots of the heat exchanger and the pipelines. Therefore, carbon accumulation was also experimentally studied at more severe conditions, namely at COG/BFG = 1.4 and doubled reaction time. In these studies, the reactor was initially filled with alumina particles. After each run, the now partially carbon-covered alumina particles were extracted from the reactor in a way that their original position is reproduced in a transparent tube (Figure 7) to present the axial carbon deposition profile.

In Figure 7, the deposit profiles along the reactor are shown with red lines marking the three reactor zones; reactor inlet, heated zone, and reactor outlet. After reforming for 60 min at 900 °C, soot-like carbonaceous deposits were formed in the heated zone, while in the reactor inlet and outlet zones no deposits were observed. Based on the kinetic simulations, we contribute this observation to molecular-growth processes starting from C_2H_4 in the hot zone. At 1100 °C, graphite-like deposits were found at the reactor inlet, the heated zone, and reactor outlet zone. The yellowish color at the lower part of the reactor outlet indicates the condensation of aromatic compounds. At temperatures above 1100 °C, carbonaceous deposits were observed at the reactor inlet zone primarily. Apparently, the temperature of the inlet zone is already high enough for significant conversion and solid carbon formation. Similar observations are described in literature for the front of the catalytic bed.[25] The carbonaceous deposits at the reactor outlet are explained by decreasing off-gas temperatures favoring reactions such as CO [Eq. (4)] and CO_2 [Eq. (5)] hydrogenation as well as the Boudouard reaction [Eq. (6)]. However, it should be noted that no complete blockage of the reactor was observed despite the rather long time-on-stream.

Herein, a dry reforming concept for the utilization of steelwork off-gases is presented and evaluated. Our exper-
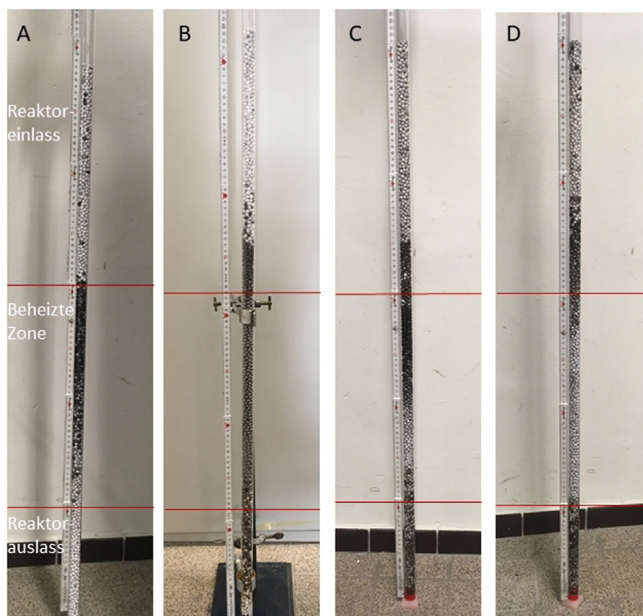

Figure 6. Coke precursors and methane presence in the simulated outlet stream at 5.5 bar.

Figure 7. Coke formation experiments at 900 °C (A), 1100 °C (B), 1300 °C (C), and 1500 °C (D) and 5.5 bar using Al_2O_3 spheres as packing material.

imental results clearly show that homogeneous dry reforming of mixtures of coke oven and blast furnace gas can be conducted at operating conditions of the regenerative heat exchanger. High conversion of CO_2 and CH_4 contained in those gases can be achieved while coke formation can be handled. The process proposed can significantly contribute to the reduction of greenhouse gas emissions from steel industry.

Experimental Section

The thermodynamic simulations were realized using the HSC Chemistry 7.1 software. The following species were considered: H_2, CH_4, CO, CO_2, H_2O, N_2, C_2H_4, C_2H_6, C_3H_8, HCN, graphitic carbon, amorphous carbon, and fullerene-type carbon (C_{60}).

For the kinetic simulations, the DETCHEM software package[26] was used and more specifically the DETCHEM^{CHANNEL} code, which models the two-dimensional parabolic flow field in a tubular reactor coupled with heat and mass transport as well as detailed chemical kinetics. The geometrical structure was chosen according to the experimental conditions of the reactor with a 40 cm long hot zone. The simulations were carried out for steady state, isothermal conditions.

For an efficient research data management including the numerical simulations and the experimental conditions and measurement results, the CaRMeN platform was used, which automatizes the work-flow of experimental-modeling studies and offers easy-to-use interfaces between reactor measurements and simulation.[27,28]

There are several detailed reaction mechanisms available in literature that could have been used for the numerical simulation of the chemical kinetics.[21,29,30,31] Four mechanisms were initially applied in the simulations of these studies. The polygeneration mechanism (PolyMech)[21] consists of 558 reactions among 83 species and was initially developed for oxidation under extremely fuel-rich conditions, an electronic version is available. The Golovichev[29] mechanism consists of 690 reactions among 130 species including C_8 hydrocarbons, which has been successfully used in the past for simulations of dry reforming at elevated pressures and temperature.[25] The Konnov[30] mechanism consists of 1231 reactions among 129 species, developed for modeling combustion processes of for example, methane and C_2–C_3 hydrocarbons. All these three mechanisms gave rather comparable results (Figures S2 and S3); the simulation results shown here are based on the PolyMech. Additionally, the AramcoMech[31] containing 3037 reactions among 581 species was initially considered but not intensively used due to very high computational costs.

The dry reforming experiments were performed in a high-temperature/high-pressure flow reactor equipped with a mass-flow-controlled system for gas admission. A controlled evaporation and mixing system is used for introduction of steam to the reactor. The flow rates of the reactants were adjusted in the range of 6×10^{-4}–0.03 $Nm^3 h^{-1}$ to account for the different ratios of COG to BFG. The ceramic reactor tube is positioned in the center of the apparatus and surrounded by argon held at the same pressure as the reacting gas in the reactor tube. The furnace is installed within a water-cooled stainless-steel pressure tank as shown in Scheme 2. The reactor can be operated at temperatures of up to 1800°C and pressures of up to 10 bar. The hot gases exiting the reactor were cooled down to condense steam. The remaining gas stream was analyzed by an online gas chromatograph (GC) with a TCD detector. For the separation of the products two columns were used; Hayesep Q for N_2/CO_2, CH_4, C_2H_4, C_2H_6 and MS 5Å for N_2 and CO. The uncertainty of the temperature measurements is ± 15°C and errors in the experimentally measured compositions were considered based on the accuracy of the Mass Flow Controllers and the GC. Some error bars for species molar fractions are included in Figure S5. In several experiments the concentration of some gases was also measured by an online FTIR
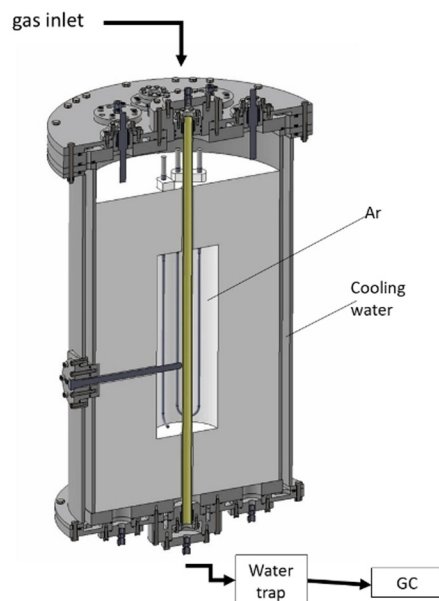
Scheme 2. Scheme of the experimental apparatus with the tubular flow reactor (greenish cylinder), which can be operated at temperatures of up to 1800°C and pressures of up to 10 bar.

analyzer (MKS Multigas 2030) to cross-check the accuracy of the GC measurements. Due to the condensation of steam, the dry gas concentration was measured. In order to simplify the investigated mixture, the COG was considered as free of oxygen and impurities (NH_3, H_2S, or HCN). As representative hydrocarbon (apart from methane) C_2H_4 was used due to its high coking tendency.[25] However, the formation of carbonaceous deposits will also be affected by other hydrocarbons contained in the off-gases. Therefore, a larger amount of C_2H_4 was chosen in the experiments than contained in COG but to have the same amount of carbon atoms present. The concentration of H_2O was chosen to be 3 vol% for COG and 5 vol% for BFG.

In the experiments to study carbon deposition, to keep the formed carbonaceous deposits at the position where they were formed Al_2O_3 spheres (Mahlperlen Schuba®MP-91, 5–7 mm) were used as inert packing material. Each experiment includes reforming reaction for 60 min for a certain temperature (900–1500°C). After cooling down, the packing material was placed in transparent tubes to examine the profiles of carbonaceous deposits.

Conflict of interest

The authors declare no conflict of interest.

[1] World Steel Association, *World Steel Assoc.* **2010**, 1–6.
[2] J. M. Bermúdez, A. Arenillas, R. Luque, J. A. Menéndez, *Fuel Process. Technol.* **2013**, *110*, 150–159.
[3] R. Razzaq, C. Li, S. Zhang, *Fuel* **2013**, *113*, 287–299.
[4] W. Uribe-Soto, J.-F. Portha, J.-M. Commenge, L. Falk, *Renewable Sustainable Energy Rev.* **2017**, *74*, 809–823.
[5] A. K. Agrawal, K. P. Kinzel, P. Bermes, C. Castagnola, in *8th Int. Congr. Sci. Technol. Ironmak.*, Vienna, **2018**.
[6] S. S. Hou, C. H. Chen, C. Y. Chang, C. W. Wu, J. J. Ou, T. H. Lin, *Energy Convers. Manage.* **2011**, *52*, 2758–2767.
[7] J.-P. Birat, in *Dev. Innov. Carbon Dioxide Capture Storage Technol.* (Ed.: M. Mercedes Maroto-Valer), Woodhead Publishing, Cambridge, **2010**, pp. 492–521.
[8] M. Modesto, S. A. Nebra, *Appl. Therm. Eng.* **2009**, *29*, 2127–2136.
[9] D. Musiał, *Combust. Sci. Technol.* **2020**, *192*, 1015–1027.
[10] W. A. Ahrendt, D. Beggs, (Charlotte N.C.), *Apparatus for Direct Reduction of Iron Using High Sulfur Gas*, **1981**, 4270739.
[11] P. Roy, N. Das, *J. Porous Mater.* **2020**, *27*, 745–754.
[12] S. Lyke, R. Moore, *US Dep. Energy* **1981**.
[13] A. Giehr, L. Maier, S. Angeli, S. A. Schunk, O. Deutschmann, *Ind. Eng. Chem. Res.* **2020**, *59*, 18790–18797.
[14] J. Shen, Z. Z. Wang, H. W. Yang, R. S. Yao, *Energy Fuels* **2007**, *21*, 3588–3592.
[15] Q. Yi, M. H. Gong, Y. Huang, J. Feng, Y. H. Hao, J. L. Zhang, W. Y. Li, *Energy* **2016**, *112*, 618–628.
[16] E. Turpeinen, R. Raudaskoski, E. Pongrácz, R. L. Keiski, *Int. J. Hydrogen Energy* **2008**, *33*, 6635–6643.
[17] D. Kim, J. Han, *Energy* **2020**, *198*, 117355.
[18] L. Deng, T. A. Adams, *Energy Convers. Manage.* **2020**, *204*, 112315.
[19] J. Lundgren, T. Ekbom, C. Hulteberg, M. Larsson, C.-E. E. Grip, L. Nilsson, P. Tunå, *Appl. Energy* **2013**, *112*, 431–439.
[20] J. Zetterholm, X. Ji, B. Sundelin, P. M. Martin, C. Wang, *Energy Procedia* **2015**, *75*, 1758–1765.
[21] S. Porras, D. Kaczmarek, J. Herzler, S. Drost, M. Werler, T. Kasper, M. Fikri, R. Schießl, B. Atakan, C. Schulz, U. Maas, *Combust. Flame* **2020**, *212*, 107–122.
[22] B. Atakan, S. A. Kaiser, J. Herzler, S. Porras, K. Banke, O. Deutschmann, T. Kasper, M. Fikri, R. Schießl, D. Schröder, C. Rudolph, D. Kaczmarek, H. Gossler, S. Drost, V. Bykov, U. Maas, C. Schulz, *Renewable Sustainable Energy Rev.* **2020**, *133*, 110264.
[23] *Soot Formation in Combustion* (Ed.: H. Bockhorn), Springer, Berlin, Heidelberg, **1994**.
[24] M. Frenklach, *Phys. Chem. Chem. Phys.* **2002**, *4*, 2028–2037.
[25] L. C. S. Kahle, T. Roussière, L. Maier, K. Herrera Delgado, G. Wasserschaff, S. A. Schunk, O. Deutschmann, *Ind. Eng. Chem. Res.* **2013**, *52*, 11920–11930.
[26] O. Deutschmann, S. Tischer, C. Correa, D. Chatterjee, S. Kleditzsch, V. M. Janardhanan, N. Mladenov, H. D. Minh, H. Karadeniz, M. Hettel, V. Menon, A. Banerjee, H. Goßler, DETCHEM Software package, 2.8 ed., www.detchem.com, Karlsruhe, **2020**.
[27] H. Gossler, L. Maier, S. Angeli, S. Tischer, O. Deutschmann, *Phys. Chem. Chem. Phys.* **2018**, *20*, 10857–10876.
[28] H. Gossler, L. Maier, S. Angeli, S. Tischer, O. Deutschmann, *Catalysts* **2019**, *9*, 227.
[29] V. I. Golovitchev, F. Tao, J. Chomiak, *SAE Tech. Pap.* **1999**, 1–15.
[30] A. A. Konnov, *Combust. Flame* **2009**, *156*, 2093–2105.
[31] C. W. Zhou, Y. Li, U. Burke, C. Banyon, K. P. Somers, S. Ding, S. Khan, J. W. Hargis, T. Sikes, O. Mathieu, E. L. Petersen, M. AlAbbad, A. Farooq, Y. Pan, Y. Zhang, Z. Huang, J. Lopez, Z. Loparo, S. S. Vasu, H. J. Curran, *Combust. Flame* **2018**, *197*, 423–438.